A Fluorescence Turn-On Mechanism to Detect High Explosives RDX and PETN

Trisha L. Andrew and Timothy M. Swager*

Department of Chemistry, Massachusetts Institute of Technology, 77 Massachusetts Avenue, Cambridge, Massachusetts 02139

Received March 19, 2007; E-mail: tswager@mit.edu

Detecting hidden explosive devices in war zones and transportation hubs is a pressing concern. Current efforts have focused on sensing three commonly used powerful explosives: 2,4,6-trinitrotoluene (TNT), 1,3,5-trinitro-1,3,5-triazinane (RDX) and pentaerythritol tetranitrate (PETN) (Chart 1). The need for ultratrace detection of these low-volatility compounds has resulted in an intense interest in fluorescence methods, and the direct detection of TNT vapor by amplifying fluorescent polymers is now an established technology.[1] However analogous examples of direct RDX or PETN detection are sparse, and current methods rely heavily on ion mobility spectrometry,[2a] mass spectrometry,[2b] and, to a lesser extent, detecting either chemically modified RDX[3a] or its degradation products.[3b] Herein we present an advance based on a molecular chemosensor (**1**) for the direct fluorescent detection of RDX and PETN.

Chart 1
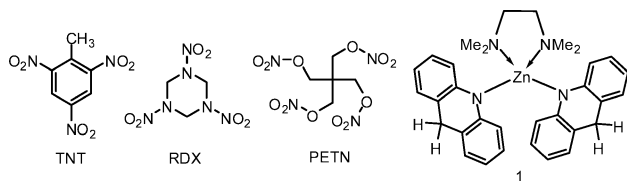
Inspired by enzymatic, NADH-mediated reduction of RDX in contaminated wastewater,[4] we sought to mimic this biological process in a fluorescence-based sensor. Initial studies targeted the NADH analogue 10-methyl-9,10-dihydroacridine (AcrH$_2$) because of its ability to form the N-methylacridinium fluorophore (AcrH$^+$) upon "H$^-$" abstraction. As seen in Figure 1B, both RDX and PETN generate the green-emitting AcrH$^+$ from the blue-emitting AcrH$_2$ upon photolysis at 313 nm in deoxygenated acetonitrile solutions, whereas TNT is ineffective.

Although AcrH$^+$ is not produced without RDX or PETN in deoxygenated solutions, it is nonetheless oxidized upon irradiation in air. Such oxygen sensitivity limits the utility of a practical chemosensor; therefore, to improve the photostability of AcrH$_2$, a
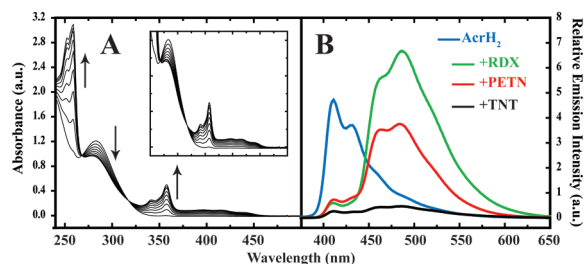
Figure 1. (A) Absorbance profile of the photoreaction of AcrH$_2$ with RDX; (B) Emission profiles of AcrH$_2$ in deoxygenated acetonitrile and its mixtures with either RDX, PETN, or TNT in degassed acetonitrile after a 60.0 s irradiation with 313 nm light. [AcrH$_2$] = 2.4 × 10^{-3} M; [explosive] = 0.012 M; λ_{ex} = 356 nm.
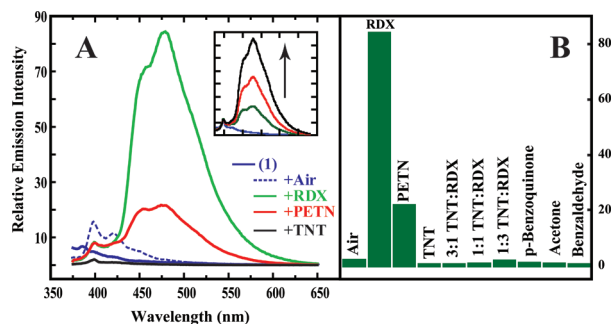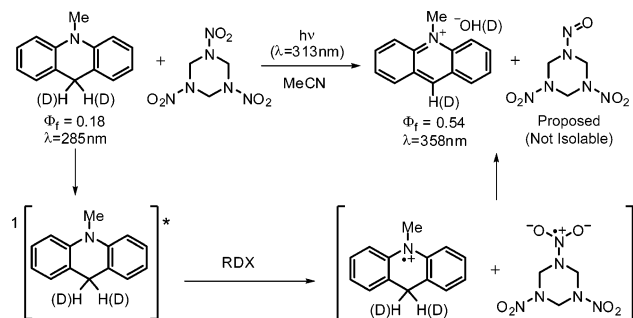
Figure 2. (A) Emission profiles of **1** in acetonitrile; **1** after a 120 s irradiation (313 nm) in acetonitrile; and mixtures of **1** and either RDX, PETN, or TNT in acetonitrile after a 30.0 s irradiation with 313 nm light. The inset shows growth of the 480 nm peak with increasing irradiation time (10 s intervals). (B) Emission intensity at 480 nm resulting from photoreaction of **1** (30.0 s irradiation times) with various explosive analytes, analyte mixtures, or select contaminants in aerated acetonitrile. [**1**] = 3.1 × 10^{-4} M; [explosive, analyte] = 0.012 M; λ_{ex} = 356 nm.

zinc analogue, **1**, was synthesized and characterized. From an initially weakly emissive, aerated solution of **1**, irradiation at 313 nm in the presence of either RDX or PETN produces an intense peak at 480 nm (Figure 2A) due to the formation of an acridine–zinc complex. This assignment is corroborated by comparing the resulting emission spectrum with that of an independently synthesized zinc–acridine complex (see Supporting Information, SI).

Irradiating **1** in the absence of an explosive analyte gives an emission band at 400 nm; however, the former 480 nm peak is not formed, even after prolonged irradiation in air. We believe that **1** slowly photooxidizes to the corresponding ketone, forming an N-substituted acridone derivative in aerated solutions (see SI). Nevertheless, a statistically significant 480 nm emission signal was observed with RDX and PETN concentrations as low as 7 × 10^{-5} and 1.3 × 10^{-4} M, respectively.

The selectivity of **1** was examined by monitoring its response to known hydride acceptors, such as p-benzoquinone and mixtures of TNT and RDX. Compound **1** is relatively unresponsive to TNT and, with TNT/RDX mixtures, the emission intensity at 480 nm increases approximately proportional to the ratio of RDX (see Figure 2B). Most strikingly, unlike the parent AcrH$_2$, **1** does not thermally reduce p-benzoquinone, and photochemical hydride transfer is found to proceed slowly. Other aliphatic and aromatic ketones and aldehydes (which are common contaminants contained within or found in the proximity of an explosive device) are also comparatively unreactive.

To better understand the mechanism involved in RDX and PETN photoreduction, we initially focused on the parent AcrH$_2$ system. As is common with NADH analogues, we anticipated one of three operative photoreduction mechanisms: a one-step hydride transfer, a two-step electron–hydrogen atom transfer or an electron–proton electron-transfer sequence.[5] Figure 1A shows a typical absorbance profile for the photoreduction reaction wherein the absorption band

Scheme 1. Proposed Photoreaction of AcrH$_2$ (AcrD$_2$) with RDX.

Figure 3. Dependence of Φ_{rxn} on [AcrH$_2$, AcrD$_2$] for the photoreduction of (A) RDX and (B) PETN. [RDX, PETN] = 6.9×10^{-4} M.

corresponding to AcrH$_2$ at 285 nm decreases with photolysis, concomitant with an increase in AcrH$^+$ absorbance at a λ_{max} of 358 nm.
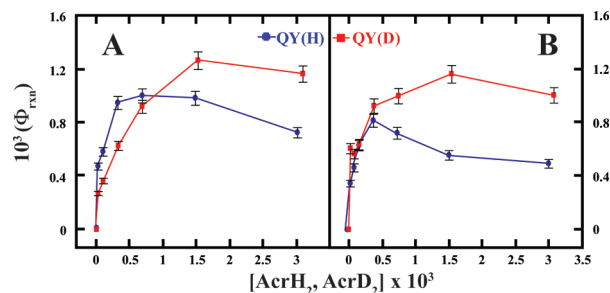
Whereas the fate of AcrH$_2$ can be followed during the course of photoreaction, the structures of reduced RDX or PETN, however, could not be easily discerned. The relatively reactive N-nitroso reaction product suggested in Scheme 1 stems from a proposed intermediate in enzymatic RDX reduction;[6] however, we have not, as yet, been able to unequivocally confirm its formation during the course of the reaction.

Nevertheless, photoreaction quantum yields (Φ_{rxn}) were obtained from a series of absorbance profiles for the reactions of RDX and PETN with AcrH$_2$ and its dideuterated analogue, AcrD$_2$ (Figure 3). The low Φ_{rxn} values (<0.1%) obtained for our system reflect the inherent inefficiency of a bimolecular photoreaction in dilute solutions and exclude any chain pathways in the photoreduction of either RDX or PETN.

At constant [RDX] and [PETN], Φ_{rxn} increases linearly with [AcrH$_2$] to a maximum value of 8.5×10^{-4} and 6.1×10^{-4}, respectively, after which it gradually decreases. A linear increase in quantum yield with increasing reactant concentration is often observed;[7] we hypothesize that the singlet excited-state of AcrH$_2$ reduces RDX or PETN (Scheme 1) and can explain, within this context, a linear increase in Φ_{rxn} with [AcrH$_2$] based on the fact that a higher AcrH$_2$ concentration increases the number of excited chromophores, which in turn leads to a greater chance of a bimolecular collision with RDX or PETN within the excited-state lifetime of AcrH$_2$. We are not, however, aware of other systems that show quantum yield saturation and subsequent decrease. We find that at sufficiently high concentrations the rate of self-quenching (the collisional deactivation of AcrH$_2$* with AcrH$_2$ (GS)) competes with analyte reduction (see SI), which lowers the overall efficiency of the photoreaction and leads to the observed decrease in Φ_{rxn}.

To distinguish between the three possible mechanisms of RDX photoreduction, we obtain a Φ_H/Φ_D value of approximately 1.3 at low [AcrH$_2$], which is consistent with a two-step electron–hydrogen atom transfer oxidation of AcrH$_2$.[7a,8] The inverse primary kinetic isotope effect (KIE) ($\Phi_H/\Phi_D = 0.77$) observed at high [AcrH$_2$] does not have literature parallels but can be explained, once again, by the self-quenching of AcrH$_2$ chromophores, in light of reports of an inverse KIE in select quenching processes.[9]

An inverse KIE is also observed at high [AcrH$_2$] for the reduction of PETN; however, a significant KIE is not observed at low [AcrH$_2$], thus implicating an electron–proton–electron transfer sequence[8] as the mechanism of PETN photoreduction.[10] In the case of TNT, photoinduced electron transfer from the singlet excited-

state of AcrH$_2$ is most probably followed by back-electron transfer and nonradiative decay to the ground state, thus accounting for the relatively inefficient production of AcrH$^+$ noted earlier. Mechanistic photophysical studies on the reaction between AcrH$_2$ and TNT and on the photoreactivity of **1** are currently in progress.

In conclusion, we have found that AcrH$_2$ is capable of selectively transferring a hydride ion equivalent to saturated nitramine and nitrate ester explosives as part of a photochemical reaction. Its photostable zinc analogue, **1**, displays an 80- and 25-fold increase in 480 nm emission intensity upon reaction with RDX and PETN, respectively. This sole example of a direct fluorescence response to RDX or PETN will enable existing fluorescence methods to detect nonaromatic high explosives, and vapor detection applications are presently being developed.

Supporting Information Available: Experimental details. This material is available free of charge via the Internet at http://pubs.acs.org.

References

(1) (a) Toal, S. J.; Trogler, W. C. *J. Mater. Chem.* 2006, *16*, 2871−2883. (b) Yang, J-S.; Swager, T. M. *J. Am. Chem. Soc.* 1998, *120*, 5321−5322.
(2) (a) Bruschini, C. *Subsurf. Sens. Technol. Appl.* 2001, *2*, 299−336. (b) For a representative example see: Cotte-Rodriguez, I.; Cooks, R. G. *Chem. Commun.* 2006, 2968−2970.
(3) (a) For a representative example see: McHugh, C. J.; Smith, W. E.; Lacey, R.; Graham, D. *Chem. Commun.* 2002, 2514−2515. (b) Jungreis, E. *Spot Test Analysis: Clinical, Environmental, Forensic, and Geochemical Applications*, 2nd ed.; J. Wiley: New York, 1997.
(4) (a) McCormick, N. G.; Cornell, J. H.; Kaplan, A. M. *Appl. Environ. Microbiol.* 1981, *42*, 817−823. (b) Bhushan, B.; Halasz, A.; Spain, J.; Thiboutot, S.; Ampleman, G.; Hawari, J. *Environ. Sci. Technol.* 2002, *36*, 3104−3108.
(5) Cheng, J-P.; Lu, Y.; Zhu, X.; Mu, L. *J. Org. Chem.* 1998, *63*, 6108−6114 and references therein.
(6) (a) Sheremata, T. W.; Halasz, A.; Paquet, L.; Thiboutot, S.; Ampleman, G.; Hawari, J. *Environ. Sci. Technol.* 2001, *35*, 1037−1040. (b) Beller, H. R.; Tiemeier, K.; *Environ. Sci. Technol.* 2002, *36*, 2060−2066.
(7) (a) Fukuzumi, S.; Fijuta, S.; Suenobu, T.; Imahori, H.; Araki, Y.; Ito, O. *J. Phys. Chem. A* 2002, *106*, 1465−1472. (b) Fukuzumi, S.; Suenobu, T.; Patz, M.; Hirasaka, T.; Itoh, S.; Fujitsuka, M.; Ito, O. *J. Am. Chem. Soc.* 1998, *120*, 8060−8068. (c) Fukuzumi, S.; Imahori, H.; Okamoto, K.; Yamada, H.; Fujitsuka, M.; Ito, O.; Guldi, D. *J. Phys. Chem. A* 2002, *106*, 1903−1908.
(8) Yuasa, J.; Fukuzumi, S. *J. Am. Chem. Soc.* 2006, *128*, 14281−14292.
(9) We propose that the rate of vibrational self-deactivation of AcrD$_2$* by AcrD$_2$ (GS) is slower than that of AcrH$_2$, thus reducing the detrimental effect of this process on Φ_D and resulting in an inverse KIE. Similarly, the vibrational deactivation of lanthanide luminescence by D$_2$O is much less efficient than H$_2$O: (i) Kropp, J. L.; Windsor, M. W. *J. Chem. Phys.* 1965, *42*, 1599−1608 and references therein. (ii) Haas, Y.; Stein, G. *J. Phys. Chem.* 1971, *75*, 3668−3677.
(10) Since RDX and PETN have different one-electron reduction potentials, it is plausible that their photoreduction mechanisms differ; see ref 5.

JA071911C